Preparation and Imaging of Intravascular High-Frequency Transducer

Xinlun Li[1], Xiaobing Li[1,*], Zheng Wu[2], Feifei Wang[2], Lixin Jiang[3], Junting Tian[1], Jiewen Zhou[1], Xiangyong Zhao[2]

1. School of Medical Instrument and Food Engineering, University of Shanghai for Science and Technology, Shanghai 200093, China.

2. Key Laboratory of Optoelectronic Material and Device, Department of Physics, Shanghai Normal University, Shanghai 200234, China.

3. Ultrasonography Department. Shanghai Renji Hospital, School of Medicine, Shanghai Jiao Tong University, Shanghai 200025, China.

***Authors to whom correspondence should be addressed**

Abstract: Intravascular ultrasound (IVUS) imaging is by far the most favorable imaging modality for coronary artery evaluation. IVUS transducer design and fabrication, a key technology for intravascular ultrasound imaging, has a significant impact on the performance of the imaging results. Herein, a 35-MHz side-looking IVUS transducer probe was developed. With a small aperture of 0.40 mm × 0.40 mm, the transducer exhibited a very wide -6 dB bandwidth of 85% and a very low insertion loss of -12 dB. Further, the *in vitro* IVUS imaging of a porcine coronary artery was performed to clearly display the vessel wall structure while the corresponding color-coded graph was constructed successfully to distinguish necrotic core and fibrous plaque via image processing. The results demonstrated that the imaging performance of the optimized design transducer performs favorably.

Keywords: High-Frequency Ultrasound Transducer; Intravascular Ultrasound Imaging

1. Introduction

Cardiovascular disease is the number one cause of death worldwide. According to data provided by the World Health Organization (WHO), in 2016, approximately 17.9 million people died from cardiovascular disease, accounting for 31% of global deaths. [1] It has been shown that atherosclerosis is an important cause of coronary syndromes. [2] Currently, the gold standard for the diagnosis of atherosclerosis is invasive coronary angiography (CAG). [3] But the CAG technique is limited to a rough assessment of luminal stenosis and does not provide information on the characteristics of the vessel wall and plaque. [4-5] In contrast, intravascular ultrasound (IVUS) can effectively enable early prediction, diagnosis, intervention, and management of vulnerable plaques and is so far the most favorable imaging modality for coronary

artery assessment. [6-7]

As the core component of IVUS, the intravascular ultrasound transducer is a high-grade medical ultrasound transducer, and many domestic and foreign medical device companies have invested their efforts in research and development. Current commercial IVUS systems have a spatial resolution of 70-200 μm in axial direction and 200-400 μm in lateral direction, which are insufficient for accurate diagnosis. [8-10] There have been many studies reported on the fabrication of IVUS high-frequency transducers. Li et al. [11] fabricated an 80 MHz IVUS transducer using a 30 μm-thick PMN-PT free-standing film that illustrated a -6dB bandwidth of 65%, and axial and lateral resolutions of 35 μm and 176 μm, respectively. Ma et al [12] used a 3-layer matching layer to increase the bandwidth of the transducer, which had a center frequency of 45 MHz and achieved a -6dB bandwidth of 61%. Zhu et al. developed a 52-MHz transducer with a BW of 61.5% using a Li-doped potassium sodium niobate (K,Na)NbO3 (KNN) thick film. [13] However, the preparation process of some composite materials is more complicated and difficult to commercialize. [14-15] Although increasing the frequency of the transducer can improve the resolution, it will have a poor penetration depth. It has become an urgent need to improve the overall performance of the transducer by balancing the frequency and resolution of the transducer.

In this paper, a center frequency 35-MHz ultrasound transducer is designed, and an optimized prepared technique is used to improve the performance of the transducer. And a data acquisition platform is designed based on the transducer measurement. The transducer resolution performance was evaluated by wire phantom imaging. Finally, the transducer was tested with an ex vivo imaging of a porcine arterial vessel.

2.Experimental

2.1Design and Fabrication of High-frequency Transducer

The aperture of the transducer was minimized to better fit the IVUS catheter. According to the KLM model, the high-frequency transducer with two acoustic matching layers and one backing layer was designed [16]. The materials and dimensions of matching layers and backing layer were optimized to provide the desired *BW* and sensitivity of the transducer. For the first matching layer, the acoustic impedance of Z_1 was controlled at 10.3 MRayls by mixing ZrO_2 particles with epoxy (EPOTEK 301, Epoxy Technology Inc. Billerica, MA). The parylene (Z_2=2.5MRayls) served as the second matching layer. The acoustic impedance of the two matching layers gradually increases the external energy projection between the piezoelectric element and the transmission medium. The PZT sample of 0.40 mm × 0.40 mm × 0.05 mm was embedded in a steel tube with an inner diameter of 0.8 mm with a backing layer made of E-solder 3022 (Von Roll Isola, New Haven, CT). The acoustic impedance of the backing layer ($Z_{backing}$) was 6.5 MRayls after cured at 60 °C for 5 h. Finally, the acoustic stack was carefully connected to a coaxial cable, and the resultant transducer was poled under a DC electric field of 1.1 kV/mm for 30 min at room temperature.

2.2 Performance Evaluation of High-frequency Transducer

The transducer performance was investigated using the pulse-echo method. A platform was designed and developed for IVUS transducer, which allowed for precise control of displacements along the *x*, *y*, and *z* directions and the rotation on the *z*-axis. The electric circuitry with a computer interface was designed

based on the LabVIEW program (National Instruments, Austin, TX) to acquire ultrasound pulse-echo signals.

A smooth steel block was used to reflect the ultrasound wave in deionized water. The distance between the transducer and steel surface was 2 mm. A pulser/receiver (DPR500, JSR Ultrasonics, a division of imaging Inc, Pittsford, NY, USA) with 5-kHz repetition rate and 50-Ω damping was used to drive the transducer. The excitation voltage was set to ~100MV in a low-pass mode. Finally, the echo signals were received by a 100-MHz oscilloscope (Dsox1102a, Key Technology, United States), and the frequency spectrum was obtained using the Fourier transformation. The *IL* of the transducer was calculated from the ratio of the received echo and the transmitted pulse, using 2.2×10^{-4} dB/mm MHz^2 to compensate the attenuation in the water [17]. The point spread function of the line model was used to evaluate the spatial resolution. A-line scan for a 6 μm-diameter tungsten wire was performed to determine the axial and lateral resolutions of the transducer.

2.3 Signal Processing and Imaging

The data acquisition and signal analysis processes for IVUS imaging are shown in Fig. 1. The transducer emitted ultrasound waves and received echo signals during the rotation. The echo signals were sampled and quantified by the data acquisition card and then transmitted to the computer. In the subsequent signal processing, the digital filtering process was performed using band-pass filtering to remove interference noises, followed by amplifying and compensating echo signals. Then, the signals were demodulated using the Hilbert transformation. Finally, the rectangular coordinates were transformed to polar coordinates to synthesize the cross-sectional images of blood vessels.

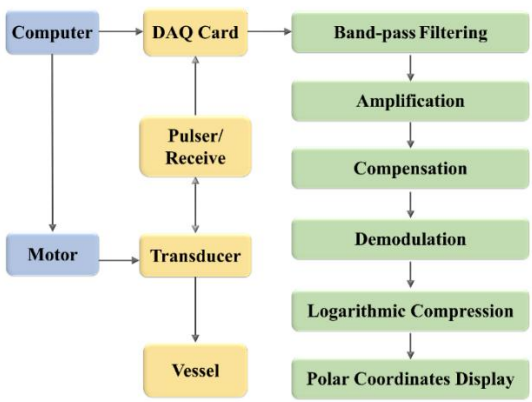

Fig. 1 Schematic of signal acquisition and imaging.

The signal acquisition device and platform are depicted in Fig. 2. The setup comprises the transducer, movable fixture, rotation setup, and electric circuits. The IVUS transducer was fixed at the front of the rotating shaft, and the electrical signals were transmitted through a slip ring to the computer when the transducer rotated along with a guidewire. The vessel sample was immersed in water and fixed at the movable fixture, which could shift in the *x*, *y*, and *z* directions independently to adjust the position precisely. Then, the IVUS transducer probe was placed into the intracavity vessel to conduct imaging experiments

including the simultaneous processes of mechanical rotation, signal transmission and collection. The radio-frequency data were digitized using a 12-bit data acquisition board (Gage Applied Technologies, Lockport, IL). Afterward, a series of signal processing was performed with the computer to produce a two-dimensional (2D) grayscale image. Based on the grayscale images, the plaques were analyzed using the pattern recognition method [18]. The region of interest was detected and the pixels were classified using feature extraction followed by color-coding.

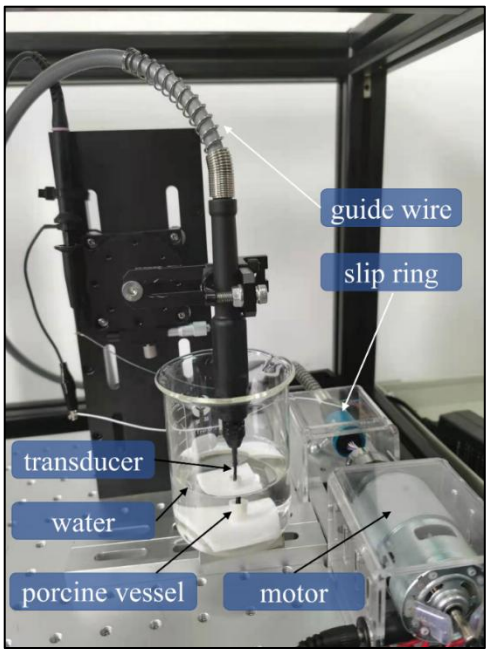

Fig. 2 Setup for ultrasound signal collection and IVUS imaging.

3. Results and analysis

3.1 Performance measurement results of IVUS Transducer

The minimum size of the IVUS catheter for current medical use is 0.87 mm, and 0.8 mm was set as the standard size in this experiment. Fig. 3(a) shows a high-frequency IVUS transducer probe. As the transducer was placed at the tip of a steel needle with an inner diameter of 0.8 mm to ensure the stable mechanical rotation in a coronary vessel for ultrasound imaging, the piezoelectric element must be as small as 0.4 mm × 0.4 mm, as depicted in Fig. 3(b). The diameter of the ultrasound beam is narrow enough to obtain a high lateral resolution.

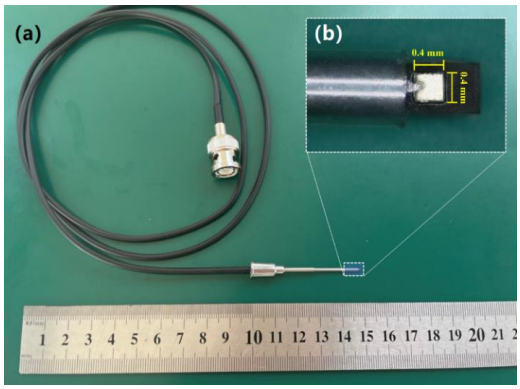

Fig. 3 photos of (a) the developed IVUS catheter and (b) transducer probe.

Fig. 4 displays the pulse-echo responses of the transducer. The frequency spectrum of the echo was analyzed using the Fourier transformation. The center frequency f_c at -6 dB and the fractional BW were determined using the following (2) and (3) [18]:

$$f_c = \frac{f_l + f_u}{2} \quad (1)$$

$$\mathrm{BW} = \frac{f_u - f_l}{f_c} \times 100\% \quad (2)$$

where f_l and f_u are the lower and upper frequencies at -6 dB. The center frequency of the transducer was 37 MHz, and the -6 dB BW was 85%. The IL was -12 dB. The detailed performances of the high-frequency IVUS transducer are listed in Table 1 [17, 19, 20]. It was found that the transducer proposed in this work exhibited much larger BW and higher sensitivity to achieve IVUS imaging, demonstrating that the improved structure is a promising way for IVUS to obtain critical fine morphological features of some plaques.

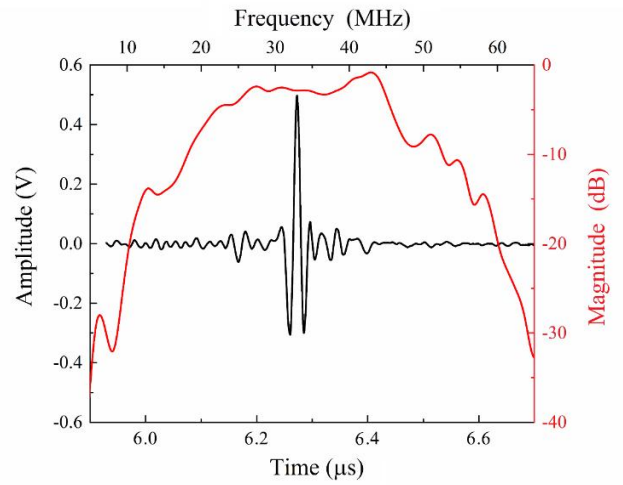

Fig. 4 Pulse-echo response of the BCHT ceramic transducer.

Table 1 Performance of high-frequency ultrasound transducers and other reported intravascular ultrasounds.

Material	f_c/MHz	-6 dB BW	IL/dB	Axial resolution/μm	Lateral resolution/μm
PZT -5H (this work)	35	85%	-12	40	250
PZT-5H [18]	40	50%	-26	38	400
PMN-PT [20]	35	54%	-	34.5	392
PMN-PT 1-3 composite [21]	34	72%		92	135

3.2 Signal processing and imaging results of IVUS Transducer

The spatial resolution of ultrasound imaging is defined as the minimum distance between two adjacent features that can be distinguished, which is a crucial factor for evaluating the capability of IVUS imaging. The high spatial resolution corresponds to the small distinguishable distance. The spatial resolution is divided into axial and lateral resolutions, which can be estimated as follows [21]:

$$R_{\text{axial}} = \frac{c}{2 f_c BW} = \frac{\lambda}{2BW} \qquad (3)$$

$$R_{\text{lateral}} = \frac{cF_{\#}}{f_c} = \lambda F_{\#} \qquad (4)$$

where c is the speed of sound, F# is the ratio of the focal length to the aperture size of the ultrasound transducer, and λ is the wavelength of the ultrasound wave. Fig. 5 demonstrates the spatial resolutions of 40 μm in the axial direction and 250 μm in the lateral direction. In the diagnosis of coronary therosclerosis, the thickness of the thin fibrous cap is considered as a reliable indicator [22]. Atherosclerotic plaques are vulnerable to rupture when the thickness of the fibrous cap is less than 65 μm. The IVUS transducer is promising to detect such thin fibrous caps.

In general, a vessel wall primarily consists of three layers: the inner tunica intima, muscular tunica media, and outer tunica adventitia. IVUS imaging is capable of providing morphological information such as lumen area, size, distribution, composition, and so on. Typical B-mode imaging of a cross-sectional porcine arterial vessel was acquired to verify the practical imaging capability of the lead-free IVUS transducer probe (Fig. 6(a)). With the image processing [17], the color-coded graph was obtained as shown in Fig. 6(b). The white arrow points to the high echo region and the reflection interface are concentrated, while the yellow arrow points to the normal region for low echo. With clearer boundary of blood vessels at high resolution, the transducer sufficiently meet the needs for IVUS imaging in clinical diagnosis.

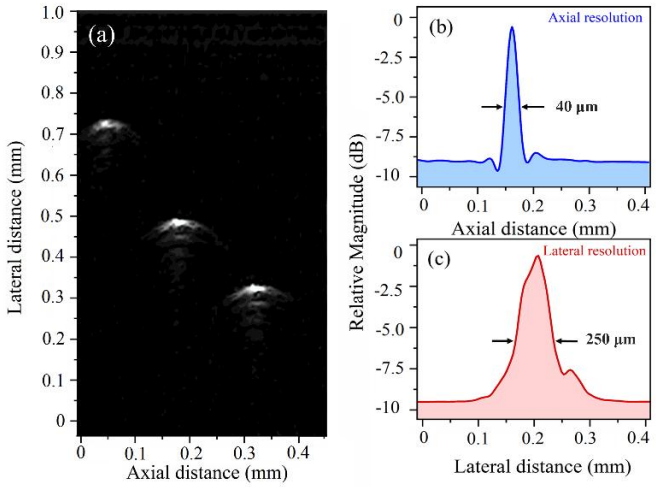

Fig. 5 (a) 6-μm tungsten wire phantom image acquired by the IVUS transducer, and the corresponding (b) axial resolution and (c) lateral resolution of the transducer.

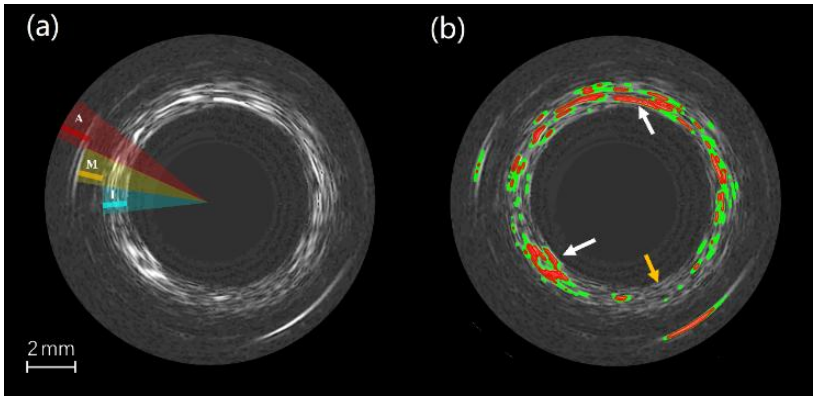

Fig. 6 (a) *In vitro* IVUS image of an in vitro porcine artery vessel, I = intima; M = media; A = adventitia. And (b) its color-coded image after feature extraction.

4. Conclusion

IVUS as a device to diagnose atherosclerotic plaques has been rapidly developed in clinical applications due to its safety and efficiency. However, the resolution of IVUS images currently used in clinical practice is low, and the acquisition of fine morphological features of some plaques is limited. This paper considers the requirements for the size and imaging resolution of the transducer for coronary imaging. The 35-MHz miniature high-frequency transducer with an effective aperture size of 0.4 mm × 0.4 mm was designed and fabricated, which exhibited excellent performance on both *BW* (85%) and *IL* (-12 dB). The IVUS imaging for a porcine artery was acquired by the developed lead-free transducer with a high axial resolution of 40 μm and a lateral resolution of 250 μm. The results show the improvement of intravascular imaging by optimizing the performance of the intravascular transducer.

References

[1] World Health Organization. Cardiovascular diseases (CVDs) [EB/OL]. (2017-05-17)[2022-04-22].

[2] Falk, E., Nakano, M., Bentzon, J. F., Finn, A. V., & Virmani, R. (2013). Update on acute coronary syndromes: the pathologists' view. European heart journal, 34(10), 719–728.

[3] Tarkin, J.M.; Dweck, M.R.; Evans, N.R.; Takx, R.A.P .; Brown, A.J.; Tawakol, A.; Fayad, Z.A.; Rudd, J.H.F. Imaging atherosclerosis.Circ. Res. 2016, 118, 750–769.

[4] de Feyter PJ, Serruys PW, Davies MJ, et al.Quantitative coronary angiography to measure progression and regression of coronary atherosclerosis. Value, limitations, and implications for clinical trials [J]. Circulation, 1991, 84(1): 412-423.

[5] Joshi FR, Lindsay AC, Obaid DR, et al. Noninvasive imaging of atherosclerosis [J]. European Heart Journal - Cardiovascular Imaging, 2012, 13(3): 205-218.

[6] Garcìa-Garcìa, H.M.; Gogas, B.D.; Serruys, P.W.; Bruining, N. IVUS-based imaging modalities for tissue characterization:Similarities and differences. Int. J. Cardiovasc. Imaging 2011, 27, 215–224.

[7] Erglis, A.; Jegere, S.; Narbute, I. Intravascular ultrasound-based imaging modalities for tissue characterisation. Interv. Cardiol. Rev.2014, 9, 151.

[8] K. Jansen, G. van Soest, A.F. van der Steen, Intravascular PhotoacousticImaging: A New Tool for Vulnerable Plaque Identification, Ultrasoundin Medicine and Biology, 2014.

[9] Elliott MR, Thrush AJ. Measurement of Resolution in Intravascular Ultrasound Images. Physiological Measurement. Nov,1996.

[10] Brezinski ME, Tearney GJ, Weissman NJ, Boppart SA, Bouma BE, HeeMR, Weyman AE, Swanson EA, Southern JF, Fujimoto JG, Assessing Atherosclerotic Plaque Morphology: Comparison of Optical Coherence Tomography and High Frequency Intravascular Ultrasound. Heart. May,1997.

[11] Li, X.; Wu, W.; Chung, Y .; Shih, W.Y .; Shih, W.-H.; Zhou, Q.; Shung, K.K. 80-MHz intravascular ultrasound transducer using PMN-PT free-standing film. IEEE T rans. Ultrason. Ferroelectr. Freq. Control 2011, 58, 2281–2288.

[12] Ma X, Cao W, Single-Crystal High-Frequency Intravascular Ultrasound Transducer With 40-mu m Axial Resolution, Ieee Transactions on Ultrasonics Ferroelectrics and Frequency Control, 67 (2020) 810-816.

[13] Zhu B, Zhang Z, Ma T, Yang X, Li Y, Shung KK, Zhou Q, (100)-Textured KNN-based thick film with enhanced piezoelectric property for intravascular ultrasound imaging, Appl. Phys. Lett., 106 (2015).

[14] Wang JS, Chen MZ, Zhao XY, et al. Fabricationand high acoustic performance of high frequency needle ultrasound transducer with PMN-PT/Epoxy 1-3 piezoelectric composite prepared by dice and fill method [J]. Sensors and Actuators A: Physical,2021, 318: 112528.

[15] Xu J, Han ZL, Wang NH, et al. Micromachined high frequency 1-3 piezocomposite transducer using picosecond laser [J]. IEEE Transactions on Ultrasonics, Ferroelectrics, and Frequency Control,2021, 68(6): 2219-2226.

[16] Krimholtz R, Leedom DA, Matthaei CL, New equivalent circuits for elementary piezoelectric transducers, Electronics Letters, 6 (1970) 398-399.

[17] Athanasiou, LS, et al. IEEE Transactions on Information Technology in Biomedicine 16(3): 391-400. (2012).

[18] K. r. Erikson, r. a. Banjavic, and P. l. carson. J. Ultrasound Med. 1, 1 (1981).

[19] Fei, C.; Yang, Y .; Guo, F.; Lin, P .; Chen, Q.; Zhou, Q.; Sun, L. PMN-PT single crystal ultrasonic transducer with half-concave geometric design for IVUS imaging. IEEE T rans. Biomed. Eng. 2017, 65, 2087–2092.

[20] Peng, J.; Ma, L.; Li, X.; Tang, H.; Li, Y.; Chen, S. A novel synchronous micro motor for intravascular ultrasound imaging. IEEE T rans. Biomed. Eng. 2018, 66, 802–809.

[21] Zhou QF, Lau ST, Wu DW, Shung KK, Prog. Mater. Sci. 56, 139 (2011).

[22] Melzer S, Ankri R, Fixler D, Tarnok A, Nanoparticle uptake by macrophages in vulnerable plaques for atherosclerosis diagnosis, J. Biophotonics, 8 (2015) 871-883.